Solid-State Compounding for Recycling of Sawdust Waste into Green Packaging Composites

Authors:

Rula M. Allaf, Mohammad Futian

Date Submitted: 2021-05-24

Keywords: wood plastic composites, cryomilling, compounding, sawdust

Abstract:

The present study explores solid-state cryomilling for the compounding of green composites. Herein, wood plastic composites (WPCs) composed of sawdust (SD) and poly(?-caprolactone) (PCL) with various compositions were prepared. Two compounding techniques, namely, extrusion and cryomilling, were utilized to prepare WPC raw material pellets and powders, respectively, for comparison purposes. Flat pressing was further utilized to prepare WPC films for testing. Morphological, structural, thermal, mechanical, and surface wettability properties were investigated. Results indicate the advantages of cryomilling in producing WPCs. Scanning electron microscopy (SEM) along with optical micrographs revealed well ground SD particles and uniform distribution in the PCL matrix. Tensile strength and elongation at break of the composites declined with increasing SD content, however, the modulus of elasticity significantly increased. Water contact angles averaged less than 90°, implying partial wetting. Visual observations and thermo-gravimetric analysis (TGA) indicated thermal stability of composites during processing. In conclusion, PCL/SD WPC is a potential candidate to replace conventional plastics for packaging applications. This would also provide a much better utilization of the currently undervalued wood waste resources.

Record Type: Published Article

Submitted To: LAPSE (Living Archive for Process Systems Engineering)

Citation (overall record, always the latest version): LAPSE:2021.0387
Citation (this specific file, latest version): LAPSE:2021.0387-1
Citation (this specific file, this version): LAPSE:2021.0387-1v1

DOI of Published Version: https://doi.org/10.3390/pr8111386

License: Creative Commons Attribution 4.0 International (CC BY 4.0)

processes

MDPI

Article

Solid-State Compounding for Recycling of Sawdust Waste into Green Packaging Composites

Rula M. Allaf [1,*] and Mohammad Futian [2]

[1] Industrial Engineering Department, German-Jordanian University, Amman 11180, Jordan
[2] Mechatronics Engineering Department, German-Jordanian University, Amman 11180, Jordan; mohammad.fetian@gju.edu.jo
* Correspondence: rula.allaf@gju.edu.jo; Tel.: +962-6-429-4524

Received: 1 October 2020; Accepted: 26 October 2020; Published: 30 October 2020

Abstract: The present study explores solid-state cryomilling for the compounding of green composites. Herein, wood plastic composites (WPCs) composed of sawdust (SD) and poly(ε-caprolactone) (PCL) with various compositions were prepared. Two compounding techniques, namely, extrusion and cryomilling, were utilized to prepare WPC raw material pellets and powders, respectively, for comparison purposes. Flat pressing was further utilized to prepare WPC films for testing. Morphological, structural, thermal, mechanical, and surface wettability properties were investigated. Results indicate the advantages of cryomilling in producing WPCs. Scanning electron microscopy (SEM) along with optical micrographs revealed well ground SD particles and uniform distribution in the PCL matrix. Tensile strength and elongation at break of the composites declined with increasing SD content, however, the modulus of elasticity significantly increased. Water contact angles averaged less than 90°, implying partial wetting. Visual observations and thermo-gravimetric analysis (TGA) indicated thermal stability of composites during processing. In conclusion, PCL/SD WPC is a potential candidate to replace conventional plastics for packaging applications. This would also provide a much better utilization of the currently undervalued wood waste resources.

Keywords: cryomilling; compounding; sawdust; wood plastic composites

1. Introduction

During the past couple of decades, substantial concerns regarding the environmental impacts, public health, and the declining availability of oil resources have directed attention towards developing more eco-friendly, green, and sustainable materials, as well as reducing and recycling wastes. Considerable research efforts have aimed to develop biodegradable and recyclable polymers and composites, particularly from renewable resources [1,2]. Natural additives regained consideration as promising fillers for developing eco-friendly, easily processed and recyclable composites, with low cost, light weight, and good mechanical properties [3–5]. The packaging industry is one of the major producers of waste; most packaging materials are discarded after product use [6]. Extensive research efforts aim to establish alternative packaging materials, including bio-based materials and sustainable fillers. Polymers under consideration include biopolymers such as chitosan, alginate, cellulosic materials, and poly (lactic acid) (PLA), as well as other biodegradable polymers including poly(ε-caprolactone) (PCL) and poly (glycolic acid) (PGA) [7–10]. Biopolymers typically face several challenges in packaging applications, related either to poor processability and/or to final properties. PLA has gained great attention in both research and commercial use. It is an aliphatic polyester derived from renewable resources such as corn [11–13]. However, PLA is relatively stiff and brittle with low deformation at break, limiting its application in packaging [12–15]. Furthermore, use of PLA in packaging would compete with food usage for agricultural resources [7]. In this investigation, PCL was

selected as a biodegradable matrix material with potential use in packaging applications [16–18]. PCL is an aliphatic polyester synthesized from nonrenewable petrochemical resources; it is biodegradable as well as recyclable. It is also semicrystalline with acceptable mechanical properties. In addition, PCL has a low glass transition temperature (−60 °C), low melting point (58–64 °C), as well as low melt viscosity, making it easily processed using either extrusion or injection processes [19–21]. PCL has been blended with PLA and chitosan to enhance the latter's flexibility and barrier properties for food packaging applications [22,23].

Large-scale application of PCL as a substitute to conventional polymers has been limited by its relatively high price and a few inferior properties. However, these properties could be enhanced through copolymerization, blending, and filling techniques [9,16]. Several studies have investigated the use of natural fibers to reinforce PCL, in addition to lowering its cost. Composites have been prepared by melt compounding [16–18,24–26] as well as solvent casting [27,28]. Ludueña et al. [17] examined the addition of different types and amounts of lignocellulosic fillers (cotton (CO), cellulose (CE), and hydrolyzed-cellulose (HCE), at 5 and 15 wt.%) to prepare PCL composite films for packaging applications. Films were prepared by melt blending, followed by compression molding. Both filler type and content influenced the crystallization, mechanical, barrier, as well as the biodegradation in soil properties of the matrix. Properties were mainly determined by the interplay of matrix crystallinity, PCL/filler interfacial strength, and filler dispersion in the matrix. Fillers accelerated the biodegradation process. Contrary to expectations, the 15 wt.% PCL/CE composite demonstrated the best performance. They concluded that the chemical treatment of cellulose in HCE was not justified, where a larger fiber aspect ratio, compatibility with matrix, and dispersion were determinant factors in the composite behavior and these were compromised by the chemical treatment. Similarly, García et al. [18] investigated the effect of almond skin filler (10, 20, 30 wt.%) on the properties of compression molded PCL composite films compounded via melt blending. Results showed enhanced mechanical and barrier properties, lower melting and crystallization enthalpies, higher crystallinity, some decrease in thermal stability, as well as higher biodegradability in composting environments compared to pure PCL. Almond skin loading of 10 wt.% has shown the best performance with potential for use in food-packaging applications. Karakus and Mengeloglu [25] manufactured PCL/wheat straw flour composites through injection molding. The addition of wheat straw resulted in improved tensile and flexural moduli as well as flexural strength; however, the tensile and impact strengths as well as the elongation at break were reduced. In a more recent study, Dhakal et al. [29] utilized date palm fibers to reinforce PCL using an extrusion process. The results showed improved mechanical properties, with a slight effect of extruder screw rotational speed. Nanocrystalline cellulose (NCC) played a significant role in reinforcing PCL. Further improvement was obtained with 10 kGy gamma irradiation treatment [16]. The treated nanocomposites demonstrated significantly increased tensile strength, tensile modulus, and elongation at break with respect to untreated PCL; furthermore, the water vapor permeability and oxygen and carbon dioxide transmission rates decreased by 25–35% [16]. However, in another study [27], a three-dimensional percolating NCC network entangled into a PCL film caused both permeability and diffusivity to increase, whereas solubility was reduced in comparison to the unfilled PCL film, which was attributed to structural defects enabling localized gas transfer in interfacial regions.

Considering the growing interest in the use of natural fillers in composites, sawdust (SD) offers a valuable candidate filler. It is a waste produced in huge amounts and is quite underutilized in various countries, where it typically serves as an animal bedding, mulch, or as a fuel, the rest being disposed of. Lately, SD has been extensively used as a filler in several virgin and recycled matrices [30,31]. In a recent study, Morreale et al. [1] investigated beech tree wood flour (WF) in a commercial blend of PLA and thermoplastic-copolyesters, known as BioFlex. WF resulted in enhanced rigidity and creep resistance without compromising tensile strength. Furthermore, reprocessing the green composite resulted in some improved properties, supporting the recyclability of such composites. Combining PCL with SD seems to be a suitable strategy for cost reduction and property enhancement. Using SD in

composites further reduces the environmental impact of the large amounts of waste produced by the furniture industry. Because of PCL's thermoplasticity, these composites can be recycled for secondary applications when they reach the end of their useful lives. Different SD contents yield a variety of colors, textures, more flexibility or more rigidity, as desired. However, several challenges exist, such as the uniform dispersion of the dust, its moisture absorption, quality, orientation, low thermal stability, and incompatibility with the PCL matrix [3,7]. In a study by Wu [24], the effect of copolymerization on the properties of PCL/WF composites was evaluated. In comparison with the PCL/WF composite, acrylic acid grafted PCL (PCL-g-AA) showed a remarkable increase in tensile strength at break and a much lower melt viscosity, due to enhanced compatibility and thus better dispersion of the WF in the PCL-g-AA matrix. Mechanical milling has been demonstrated to enhance compatibility, dispersion, and thus properties of blends and composites [32–34]. For that purpose, this study presents investigations on the fabrication of PCL/SD wood plastic composites (WPCs) via a solid-state route, namely, cryomilling. The process-ability of the WPC, i.e., the ability to fabricate products with good physical integrity, was examined up to the highest feasible filling level. Furthermore, cryomilling was compared to extrusion for effective compounding to disperse the SD in the PCL matrix without compatibilizers. Samples were produced via hot-pressing. Mechanical, structural, thermal, as well as hydrophilicity properties were investigated.

2. Materials and Methods

2.1. Materials

Capa® 6506, a commercial grade poly (ε-caprolactone) powder, was kindly supplied by Perstorp UK Limited (Lowton, UK). Capa® 6506 manufacturer's reported properties include a molecular weight of 50,000 g/mol, a density of 1.1 g/cm^3 (at 60 °C), a melting temperature of 58–60 °C, a melt flow index (MFI) of 11.3–5.2 g/10 min (2.16 kg at 160 °C), and a particle size of less than 600 µm. Whitewood SD particles collected from the engineering workshop at the German Jordanian University were utilized as a filler. The SD was sieved to a particle size < 1 mm. SEM images revealed the presence of particles in a wide range of shapes and size (~10 to 850 µm). Before compounding the mixture samples, SD was dried in a Heratherm oven (Thermo Fisher Scientific, Waltham, MA, USA) at 80 °C for 48 h to reduce moisture.

2.2. PCL/SD Compounding and Sample Preparation

PCL/SD composite sheets were fabricated via hot pressing in a bench-top hydraulic laboratory press (Carver, Inc., Wabash, IN, USA). Before processing, different formulations of PCL/SD were manually mixed. Then, mixtures were compounded via two different techniques, namely extrusion and cryomilling, to prepare PCL/SD pellets and powders, respectively. Extrusion was executed on a laboratory scale DSE-20B twin-screw extruder (Laryee Technology Co., Ltd., Beijing, China) with a length/diameter ratio of 40 and a screw diameter of 21.7 mm utilizing a 3 mm circular die to form the extrudate. After numerous trial and error experiments, the extrusion parameters were set at a screw speed of 24 rpm, feeder speed of 8 rpm, and barrel zones temperature from 70 °C to 90 °C. The composite wires were cooled down in a water-cooling bath and then pelletized (approx. 3 mm in length) to prepare WPC pellets for hot pressing. Cryomilling was accomplished in a Retsch Cryomill (Retsch GmbH, Haan, Germany). Powders were filled in a 25 cm^3 grinding jar with five 10 mm stainless steel milling balls and then milled for 27 min at a frequency of 30 Hz. Thereafter, powders were stored in the oven at 40 °C to reduce moisture before melt processing. Subsequently, sheets were obtained by compression molding at 100 °C. Pellet and powder samples (1.5 g) were sandwiched between two Teflon sheets and hot pressed utilizing a 50 kN force for 5 min. Next, samples were cooled down to room temperature, and later specimens were cut using punches for characterization.

2.3. Sample Characterization

Scanning electron microscopy (SEM): A Vega 3 scanning electron microscope (TESCAN, Brno, Czech Republic) was used to study the morphologies of cryomilled powders and fabricated sheets. Samples were mounted on the SEM sample holder using aluminum stubs with double-sided carbon tape. Before imaging, samples were sputter coated with a thin layer of platinum in an SC7620 Sputter Coater (Quorum Technologies Ltd., Lewes, UK).

X-ray diffractometry (XRD): XRD measurements on cryomilled powder samples were carried out on a D2 Phaser (Bruker, Karlsruhe, Germany) powder diffractometer at room temperature utilizing Cu Kα radiation (1.54056 A, 30 kV, 10 mA). Data were collected at a scanning rate of 0.05 °/sec from 0 to 40 (°2θ).

Differential scanning calorimetry (DSC): The thermal behavior of cryomilled powders was investigated using DSC in a Q20 DSC (TA Instruments, New Castle, DE, USA). Specimens of ~10 mg weight underwent a first heating scan from 30 °C up to 180 °C, a cooling scan to 30 °C, and eventually a second heating scan up to 180 °C. The heating and cooling rates were set at 10 °C/min and the hold time between scans at 2 min. Nitrogen was used as the purge gas through the DSC cell at a flow rate of 50 cm^3/min. Data were analysed using TA Universal Analysis Advantage Software v5.5.3 to determine transition temperatures and enthalpies. The degree of crystallinity of PCL (X_c) was determined by the fusion enthalpy method, using the following equation [35]:

$$X_c(\%) = \frac{\Delta H_m - \Delta H_c}{\Delta H_{m,100\%}} \times \frac{1}{wt_{PCL}\%/100} \times 100\%$$

where ΔH_m, ΔH_c, and $wt_{PCL}\%$ designate the measured melting enthalpy, cold crystallization enthalpy, and weight percentage of PCL in the sample, respectively. The value of the melting enthalpy of 100% crystalline PCL ($\Delta H_{m,100\%}$) used was 139.5 J/g [36]. Second heating scans were analyzed corresponding to materials' properties with erased previous thermal histories.

Thermogravimetric analysis (TGA): TGA was performed on cryomilled powder samples using a Netzsch TG209 F1 Libra TGA (Netzsch, Selb, Germany) machine. Samples (12.00–15.00 mg) in tared open aluminium pans were subjected to heating from 30 °C to 300 °C at a heating rate of 10 °C/min under a nitrogen gas purge at 20 cm^3/min and 10 cm^3/min through the furnace and TGA head, respectively. Proteus®-61 Software was used to analyze the thermogravimetric (TG) curves for mass loss at 300 °C and onset degradation temperature at 0.5% mass loss ($T_{0.5\%}$).

Tensile properties: sheet samples were cut into rectangular specimens (6 mm width × 80 mm length). Thickness was measured from at least five random locations on each sheet using a micrometer (Mitutoyo, Kawasaki, Japan) with a 0.01 mm resolution. Then, the mean thickness value was used for the succeeding calculations. A universal tensile testing machine (Testometric Co. Ltd., Rochdale, UK) was utilized to carry out the tensile tests. Specimens (35 mm gauge length) were tested at a crosshead speed of 1 mm/min and at room temperature. Five specimens were tested per composition. OriginPro 8.5 software (OriginLab Corporation, Northampton, MA, USA) was used to evaluate Young's modulus of elasticity, tensile strength, and elongation at break from resultant force-elongation data. Statistical analysis of results was performed with Minitab software (Version 17.0, State College, Pennsylvania, USA). Differences between means were assessed based on an unpaired Student's *t*-test at a *p*-value < 0.05 significance level.

Water contact angle (WCA): A home-made goniometer was used to examine the surface hydrophobicity of the fabricated sheets by the sessile drop contact angle method. The sheet was fixed on a well-leveled home-made plastic platform. Droplets of distilled water (~7 μL) were placed on top of the sheet surface using a micrometer syringe. Pictures of the droplets were acquired using a digital camera. A drop-shape analysis software was used to measure the contact angle via the tangent method. Tests were carried out on at least two samples at two different locations for each composition and the average was calculated.

3. Results and Discussion

3.1. Properties of Compounded PCL/SD

Conventional fabrication techniques to produce polymer composites encompass melt blending, solution mixing, and in situ polymerization. Extrusion, which is a melt mixing technology, has been the dominant commercial compounding technique. Other compounding techniques include solid-state blending technologies. The present study investigated solid-state cryomilling compared to extrusion for compounding PCL with SD to produce WPC sheets for packaging applications. The compounding-ability of the WPC was examined up to the highest practical SD filling level. Powders were cryomilled up to 70 wt.% SD; however, extrusion failed beyond 40 wt.% SD. Figure 1 shows an extruded sample with 50 wt.% SD content. The extrudate had a disintegrating physical appearance and was too brittle for continuous extrusion and handling. Digital camera photographs, as well as SEM images of cryomilled powders, in addition to raw powders are presented in Figure 2, while Figure 3 shows extruded pellets. Figure 2 clearly demonstrates the grinding and compounding effects of this solid-state process, where SD was ground into a fine powder, which was completely and uniformly compounded with the PCL particles. In reference to the composite color, the powder color resembled that of SD, with color showing little changes as the SD content increased. Furthermore, it was evident that the composite powder size decreased with higher SD content, with SD acting as a grinding agent. On the other hand, the extruded pellets had darker brown colors with higher darkness as SD content increased. It was also noted that pellet size increased with SD content at the same extrusion parameters.

Figure 1. Poly(ε-caprolactone (PCL)/ sawdust (SD) extruded wire with SD content of 50 wt.%.

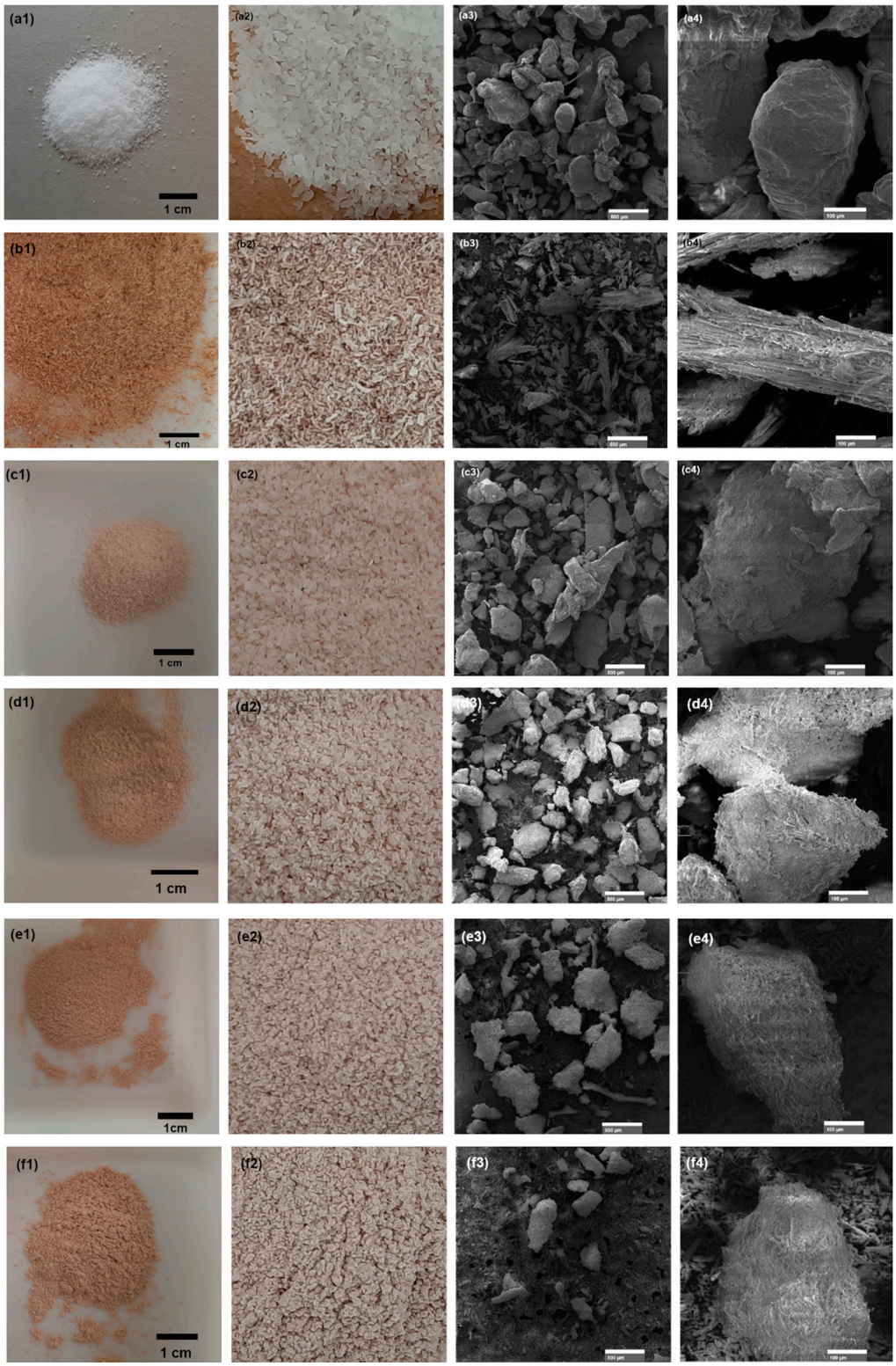

Figure 2. Images of PCL/SD powders: (**a**) pure PCL, (**b**) pure SD, (**c**–**f**) cryomilled PCL/SD powders with SD content of 10, 30, 50, and 70 wt.%, respectively. Subscripts 1 and 2 refer to digital camera photographs with 4× magnification for 2; while subscripts 3 and 4 refer to SEM micrographs with white scale bars of 500 and 100 µm, respectively.

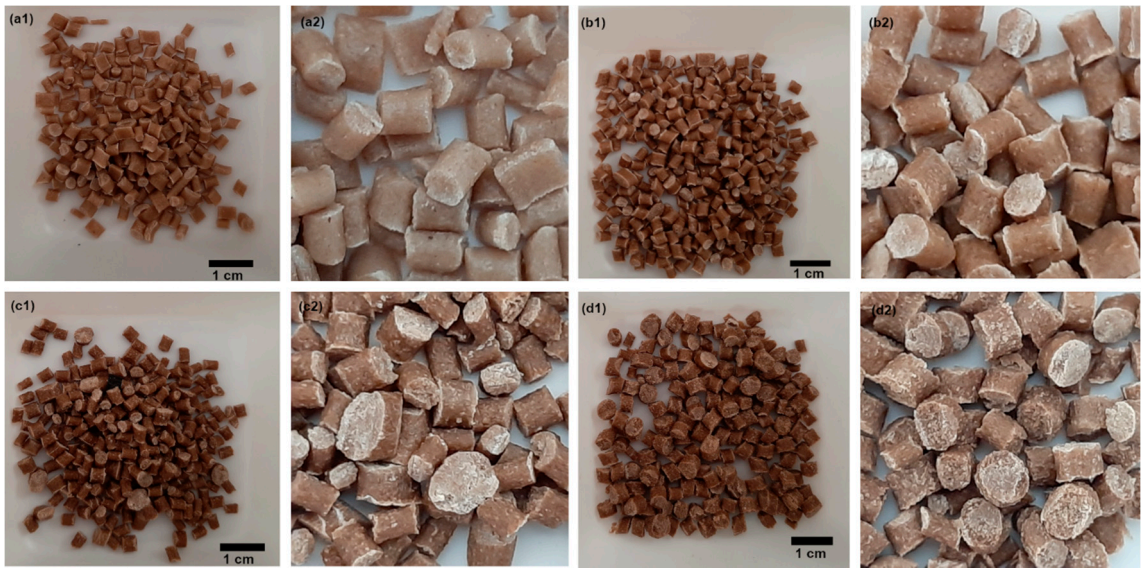

Figure 3. Images of PCL/SD extruded pellets with SD content of (**a**–**d**) 10, 20, 30, and 40 wt.%, respectively. Subscripts 1 and 2 refer to digital camera photographs with 4× magnification for 2.

XRD patterns of cryomilled composite powders prepared at different compositions are shown in Figure 4. The neat PCL pattern shows strong characteristic peaks at 21.4 and 23.8 °2θ. Through fitting the XRD peaks by Gaussian functions, the % crystallinity of PCL was calculated as 42%. The neat SD pattern shows a typical pristine wood pattern, with low intensity and broad diffraction peaks at ~15 and 22 °2θ, associated with cellulose [37]. The 10 wt.% SD composite pattern almost overlaps with the neat PCL pattern. Other composite patterns (20 wt.% till 70 wt.%) resemble that of PCL with around a 35% reduction in intensity for peaks and minor peak position shifts, which may be attributed to blending and experimental error. Results do not indicate any structural or chemical changes due to the compounding technique.

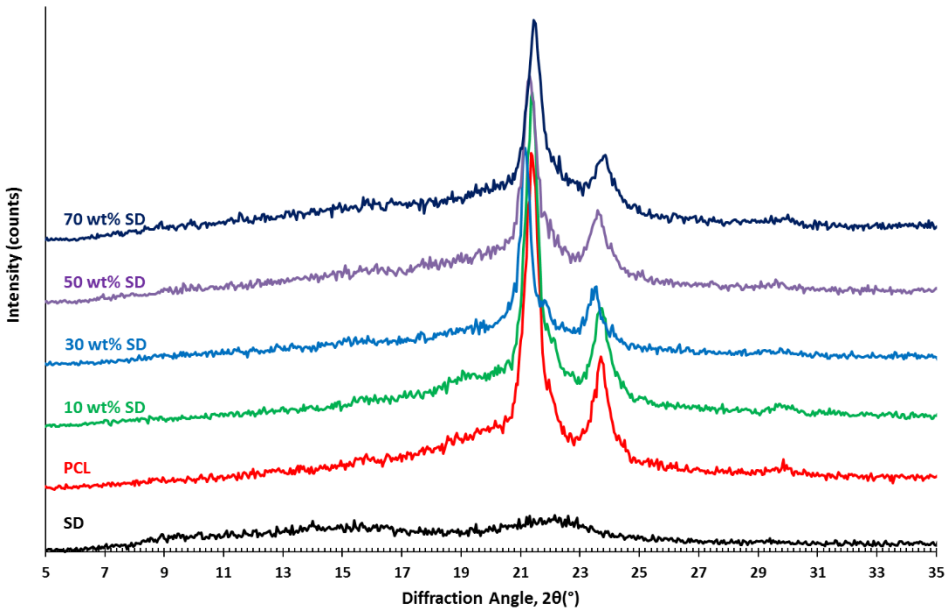

Figure 4. XRD patterns of cryomilled PCL/SD composite powders as function of composition.

DSC and TGA tests for PCL/SD (10 and 30 wt.% SD) composites were performed to compliment the XRD results and assure the thermal stability of the composites during processing and testing.

Neat PCL exhibits well-defined melting peaks (thermograms not shown here), with a peak melting temperature, T_m of 58 °C, and fusion enthalpy, ΔH_m of 56.6 (0.1) J/g. Calculated PCL % crystallinity from DSC was 41%. DSC heating thermograms for PCL/SD (10 and 30 wt.%) are shown in Figure 5. Extracted heats of fusion and peak melt temperatures are summarized in Table 1. It is evident that there is a substantial difference between the first heating scan thermogram and the second for the 10 wt.% SD composite, with the first indicating a higher meting point and fusion enthalpy. This may explain the XRD results, where solid-state blending of up to 10 wt.% SD via cryomilling did not affect the PCL crystallinity. While the 30 wt.% SD showed minor differences between its scans and the second scan of the 10 wt.% SD sample. Based on second heating scans after erasing the samples' thermal histories, addition of SD up to 30 wt.% resulted in a 1.5 °C decrease in the PCL melt temperature and decreased fusion enthalpy, indicating a ~39% reduction in crystallinity. Similarly, Wu declared an almost linear decrease in melt temperature (from 62.5 to 60.2 °C) with increasing WF content up to 30 wt.%, almost stabilizing thereafter up to 50 wt.% [24]. Furthermore, Wu declared a reduced fusion enthalpy with a higher WF content, which Wu attributed to lower percentage crystallinities as the WF content increased resulting from lower polymer chain movement and hydrophobic interactions. However, our DSC results indicate an exothermic peak occurring right in front of the endothermic melting peak affecting the accuracy of our calculations. Similarly, Ludueña et al. reported a reduced crystallinity and melting temperature upon addition of up to 15 wt.% cellulose to PCL, which they attributed to heterogeneous nucleation [17].

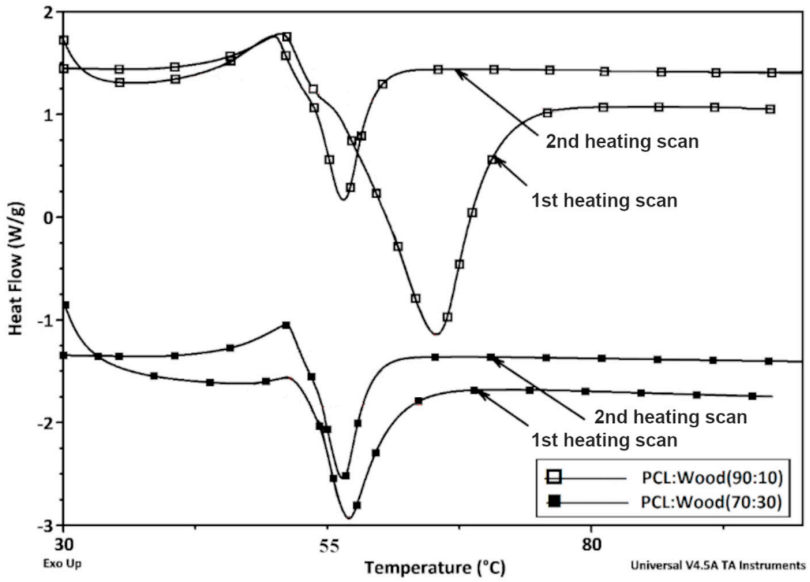

Figure 5. Differential scanning calorimetry (DSC) thermograms of cryomilled PCL/SD composite powders with SD content of 10 and 30 wt.%.

Table 1. Main thermal properties of PCL/SD composites with 10 and 30 wt.% SD content obtained by DSC.

SD Content	Melt Peak Temperature, T_m (○C)	Melt Enthalpy, ΔH_m (J/g)	Degree of Crystallinity, X_c (%)
1st heating scan			
10 wt.%	65.3	59.0	40
30 wt.%	57.0	28.5	25
2nd heating scan			
10 wt.%	56.5	31.3	25
30 wt.%	56.5	25.6	26

Previous TGA results indicated that PCL is thermally stable up to ~338 °C, with a peak degradation temperature of 404 °C and 1 wt.% mass loss at 300 °C. Wood components (hemicellulose, cellulose and lignin), on the other hand, degrade in a complex process at lower temperatures. Below 100 °C, any weight loss is associated with residual moisture. From 100 °C to 200 °C, wood dehydrates and with prolonged exposure to high temperatures, it becomes charred. Significant pyrolysis starts at ~200 °C, with hemicellulose, cellulose, and lignin components depolymerizing in the temperature ranges of ~200–300 °C, 250–370 °C, and 225–500 °C, respectively [18,38,39]. TGA thermograms for PCL/SD (10 and 30 wt.%) are shown in Figure 6. The results of the TGA evaluations of the onset loss temperature ($T_{0.5\%}$) and percentage mass loss at 300 °C are listed in Table 2. The addition of 10 wt.% SD had insignificant effects on PCL's thermal stability; 30 wt.% resulted in the earlier onset of degradation. However, both composites show good thermal stability up to 300 °C. Since PCL is typically processed in the temperature range of 80–150 °C [17,18,24,40,41], addition of SD would decrease its thermal stability, but will not compromise its processing and applications in the packaging industry. Furthermore, these outcomes assure no degradation during DSC testing. These results are in good agreement with those attained by García et al. [18] for PCL/almond skin (AS) composites. At 10 wt.% AS content, PCL maintained its thermal stability with an initial degradation temperature of ~381 °C, compared to that of pure PCL of ~385 °C. The addition of 30 wt.% AS promoted earlier degradation at ~272 °C, which they attributed to a lower matrix homogeneity at that formulation. Reduced PCL thermal stability may be explained by the generation of acidic products from hemicellulose and cellulose decomposition, promoting random scission of PCL's ester linkages [42]. Similar behavior was also reported by Liminana et al. [39] for biodegradable poly (butylene succinate (PBS)/almond shell flour (ASF) composites. PBS/ASF composites (up to 50 wt.% ASF) were thermally stable up to 250 °C; noting low PBS processing temperatures from 130 to 140 °C.

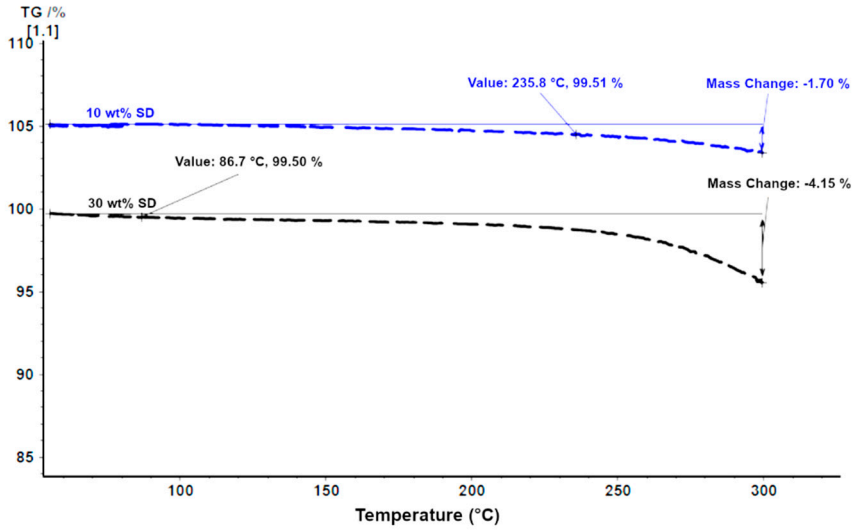

Figure 6. Thermo-gravimetric analysis (TGA) thermograms of cryomilled PCL/SD composite powders with SD content of 10 and 30 wt.%.

Table 2. Main thermal properties of PCL/SD composites with 10 and 30 wt.% SD content obtained by TGA.

SD Content	0.5% Weight Loss Temperature ($T_{0.5\%}$) (°C)	Mass Loss at 300 °C (%)
10 wt.%	236	1.7
30 wt.%	87	4.2

3.2. Properties of PCL/SD Composite Sheets

Compounded powders and pellets were consolidated by flat pressing to produce WPC sheets. Sample thicknesses, whether compounded via cryomilling or extrusion, ranged from 0.13 mm to 0.17 mm, increasing with SD content up to 50 wt.%. However, the 70 wt.% cryomilled samples had very little fluidity, which resulted in an average thickness of 0.40 mm. Visual inspections showed uniform colors for all cryomilled formulations, implying homogeneous SD dispersions in the PCL matrix (Figure 7a). Similar results were seen for the extruded ones; however, SD particles were still evident in the sheets (Figure 7b). Similar images were presented by Annandarajah et al. for agave fiber (5, 10, 20, and 30 wt.%) reinforced polypropylene, linear low density, and high density polyethylene composite films prepared via extrusion [43]. It is also worth mentioning that some samples suffered dewetting and melt flow marks. The surface morphology of the composite sheets was further studied by scanning electron microscopy. Figure 8 shows SEM micrographs for cryomilled sheets. Images implied homogeneous SD dispersions, with some dispersed agglomerates observed, being more evident in PCL with 70 wt.% SD. Ludueña et al. reported similar results for PCL based composites containing different lignocellulosic filler types up to 15 wt.% content [17]. In comparison, Garcia et al. reported less efficient dispersion of almond shell (AS) particles inside the PCL matrix for the 20 and 30 wt.% formulations [18]. Filler agglomeration has been attributed to the poor polymer/filler compatibility [17,18]. In contrast, solid-state cryomilling has shown enhanced dispersion, grinding, and compounding of the filler and the matrix.

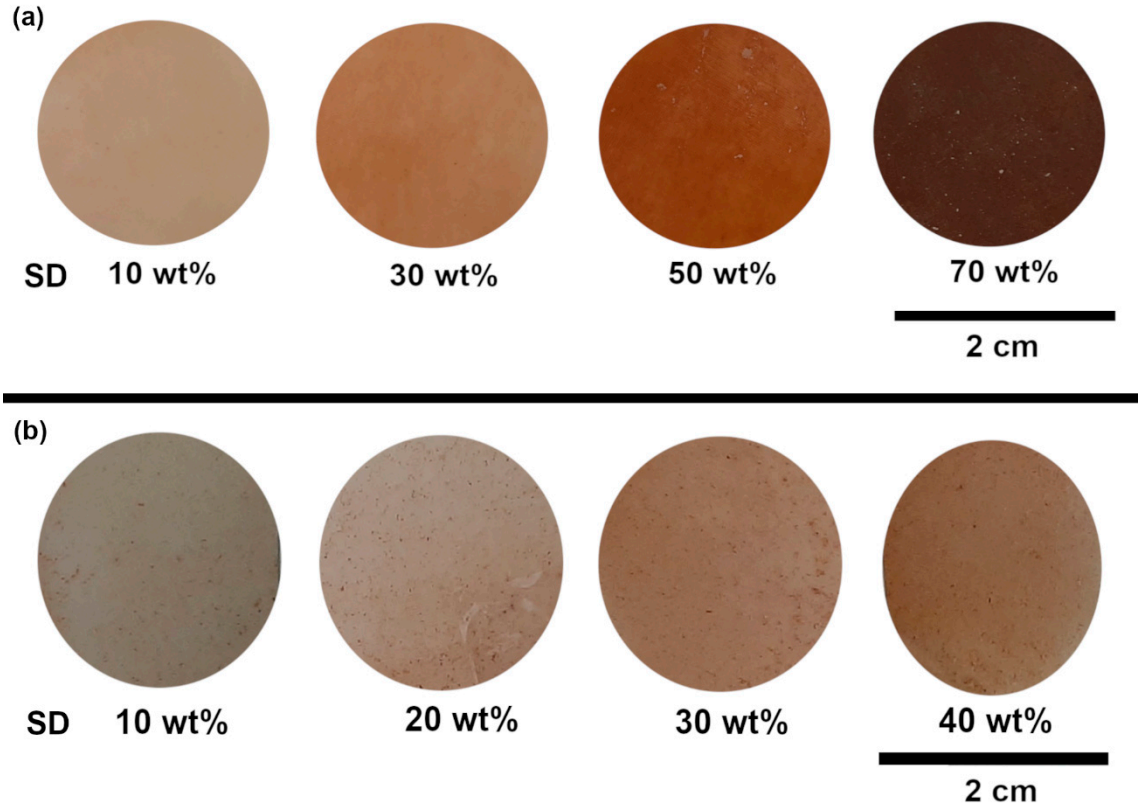

Figure 7. PCL/SD flat-pressed sheets (**a**) compounded via cryomilling with SD content increasing from 10 till 70 wt.%, respectively; (**b**) compounded via extrusion with SD content increasing from 10 till 40 wt.%, respectively.

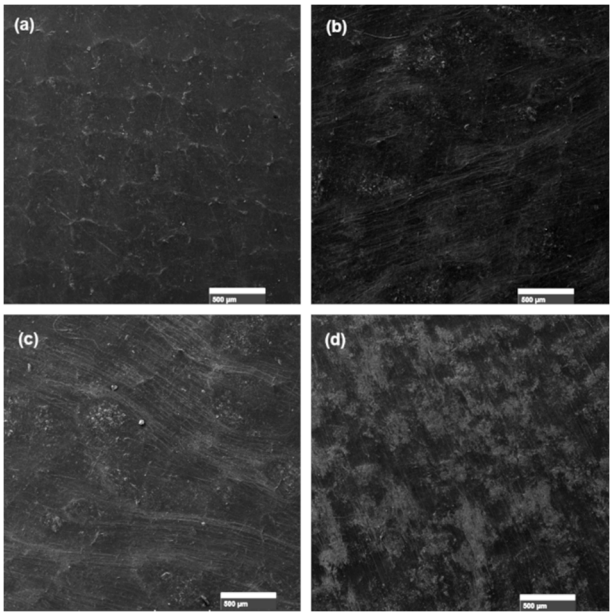

Figure 8. SEM micrographs of PCL/SD flat-pressed sheets compounded via cryomilling with (**a**–**d**) SD content of 10, 30, 50, and 70 wt.%, respectively. White scale bars measure 500 μm.

The effects of SD content and processing route on the tensile properties of the composites are illustrated in Figure 9. Sheets with 60 wt.% SD content and beyond were brittle to cut, therefore were not tested. Compared to pure PCL with a tensile modulus of 188 (46) MPa, tensile strength of 27.0 (1.6) MPa, and strain at break of 8.96 (0.26) mm/mm; addition of SD resulted in significant changes to the mechanical properties. Similar trends were seen for both compounding techniques, where the tensile modulus increased almost linearly from 10 wt.% up to 40 wt.% SD, with the cryomilled 50 wt.% SD sample showing a substantial increase. Tensile strength showed a considerable decrease compared to pure PCL (~64% decrease with as little as 10 wt.% SD), with small decline with increasing SD content. Finally, strain at break showed a substantial decrease (~95%) compared to pure PCL, and then decreased linearly with increasing SD content. Both compounding techniques showed insignificant differences between moduli and strength at each SD content. However, cryomilling showed significantly enhanced ductility, as evident with strain at break values, suggesting a possible compatibilization effect between PCL and SD [39] and good potential for their use in flexible packaging applications. The effect of molding temperature was also investigated. Cryomilled samples were pressed at 150 °C; results (Table 3) showed reduction in all properties with increasing temperature. Thereby indicating better processability at lower molding temperatures.

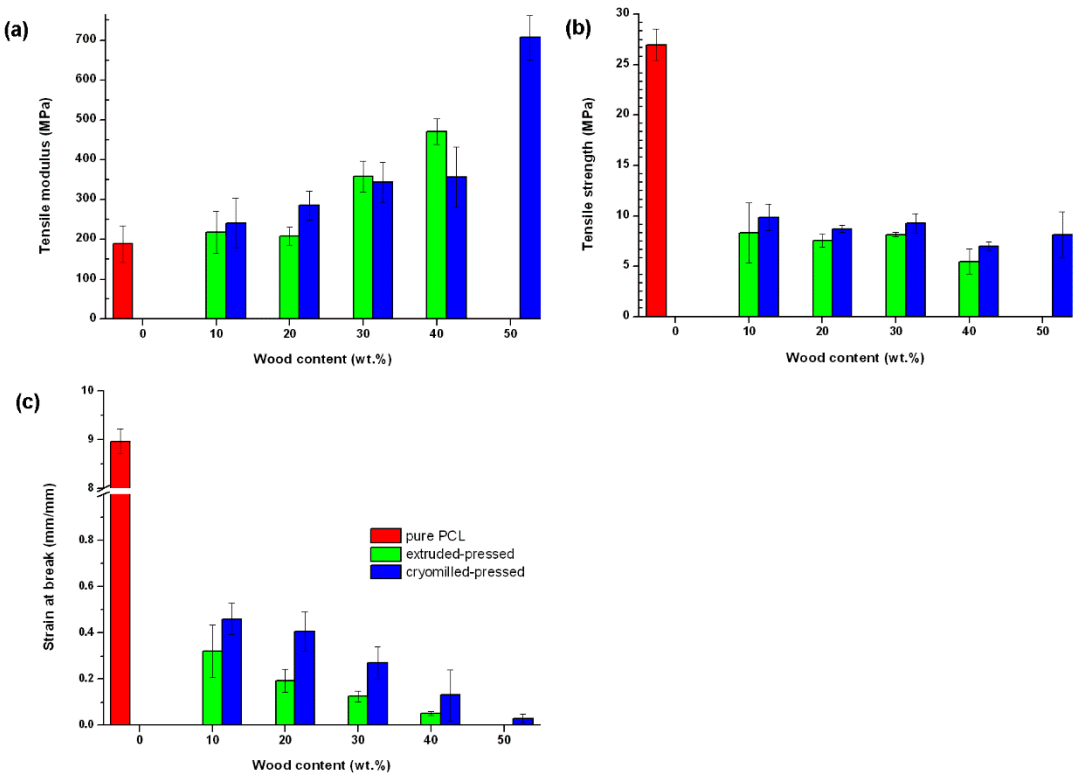

Figure 9. Tensile properties of PCL-SD wood plastic composites (WPC) compounded via two techniques, namely cryomilling and extrusion: (**a**) tensile modulus, (**b**) tensile strength, and (**c**) strain at break as function of SD content.

Table 3. Average tensile properties for the cryomilled PCL/SD WPCs flat pressed at different temperatures.

SD Content		Tensile Modulus (MPa)			Tensile Strength (MPa)			Strain at Break (%)		
		10 wt.%	30 wt.%	50 wt.%	10 wt.%	30 wt.%	50 wt.%	10 wt.%	30 wt.%	50 wt.%
Molding Temperature	100 °C	318 (80)	493 (79)	707 (55)	14.6 (2.9)	10.3 (1.5)	8.1 (2.3)	60.2 (48.3)	6.4 (2.4)	2.6 (1.8)
	150 °C	269 (17)	337 (168)	707 (133)	11.1 (1.3)	8.2 (1.7)	6.8 (0.5)	22.7 (11.6)	8.3 (4.1)	1.5 (0.8)

To establish the utility of our PCL/SD composites for flexible packaging, mechanical properties data from several literature reports are summarized in Table 4. It is clear that many polymers with a wide range of properties are investigated and/or utilized for packaging applications. Homopolymers, co-polymers, blends, and composites with various additives have been examined. Poly(ethylenes) (LLDPE, LDPE, HDPE), poly(propylene) (PP), poly(ethylene terephthalate) (PET), and poly(vinyl chloride) (PVC) are the most commonly used conventional polymers in the flexible packaging industry [44]. Many green alternatives, especially biocomposites have been explored and/or commercialized. PCL biocomposites have been recently advocated for food packaging applications [17,18]. The mechanical properties of our PCL/SD composites follow the general trends in relation to fiber incorporation, that is, tensile strength and elongation at break decrease while the modulus of elasticity increases. Furthermore, these properties seem reasonable for flexible packaging applications. Nevertheless, the literature reports show enhanced properties with the addition of coupling agents, compatibilizers, and/or with matrix or filler treatment. Thus, addition of a compatibilizer or SD treatment could further improve our properties. However, this would add to the cost and complexity of the processing, not to forget the potential environmental problems.

Table 4. Mechanical properties of polymers and biocomposites from literature reports.

Ref	Fiber Type and Content	Matrix	Fabrication Method [1]	Modulus of Elasticity (MPa)	Tensile Strength (MPa)	Strain at Break (%)
[17] [3]		PCL (0.3–0.5 mm) [2]	Mixer-Press	330 ± 12	19.0 ± 0.5	897 ± 48
[17] [3]	CO [6] (15 wt.%)	PCL	Mixer-Press	488 ± 22	14.2 ± 0.3	188 ± 80
[17] [3]	CE [6] (15 wt.%)	PCL	Mixer-Press	497 ± 40	19.4 ± 0.9	410 ± 65
[17] [3]	HCE [6] (15 wt.%)	PCL	Mixer-Press	407 ± 23	12.1 ± 0.7	385 ± 72
[18] [3]		PCL (210 μm) [2]	Mixer-Press	335 ± 8		68 ± 7
[18] [3]	AS [6] (10 wt.%)	PCL	Mixer-Press	392 ± 8		38 ± 1
[18] [3]	AS (30 wt.%)	PCL	Mixer-Press	280 ± 4		18 ± 1
[39]		PBS [6]	Extrusion -Injection	417 ± 21	31.5 ± 0.9	215.6 ± 16.5
[39]	ASF [6] (30 wt.%) [4]	PBS	Extrusion -Injection	790 ± 56	14.8 ± 0.5	6.3 ± 0.9
[39]	ASF (10 wt.%) + MLO [6] (1.5 wt.%)	PBS	Extrusion -Injection	561 ± 29	24.6 ± 0.2	17.0 ± 0.6
[39]	ASF (30 wt.%) + MLO (4.5 wt.%)	PBS	Extrusion -Injection	535 ± 51	13.8 ± 0.3	25.8 ± 1.0
[39]	ASF (50 wt.%) + MLO (7.5 wt.%)	PBS	Extrusion -Injection	364 ± 47	7.1 ± 0.2	16.4 ± 1.0
[45] [3,4]		PP [6]		1300	35	
[45] [3,4]	Ramie fiber (10 wt.%) + PP-g-MA (3 wt.%)	PP		1400	42	
[45] [3,4]	Ramie fiber (30 wt.%) + PP-g-MA [6] (3 wt.%)	PP		2250	66	
[45] [3,4]		HDPE [6]		475	17.5	
[45] [3,4]	Date palm trunk fiber (30 wt.%) + PP-g-MA (2 wt.%)	HDPE		975	18	
[45] [3,4]		LDPE [6]		130	7.6	
[45] [3,4]	Bleached date palm leafs (28 wt.%)	LDPE		390	6.8	
[45] [3,4]		PP		800	27.5	
[45] [3,4]	Bleached date palm leafs (28 wt.%)	PP		675	17	
[45] [3,4]		PC [6]		1100	67.5	
[45] [3,4]	Alkali treated pineapple leaf fiber (20 wt.%)	PC		2000	71.0	
[2]		LLDPE	2-Roll mill-Press	1160(200)	21.11(2.56)	-
[2]	Birch fibers (30 wt.%)	LLDPE	2-Roll mill-Press	2460(230)	33.04(1.85)	5.90(0.92)
[2]	Birch fibers (30 wt.%) + MAPE [6] (3 wt.%)	LLDPE	2-Roll mill-Press	3300(200)	40.09(1.59)	4.35(0.53)
[2]		HDPE	2-Roll mill-Press	1270(70)	22.00(0.86)	-
[2]	Birch fibers (30 wt.%)	HDPE	2-Roll mill-Press	2940(130)	34.04(1.13)	3.50(0.39)
[2]	Birch fibers (30 wt.%) + MAPE (3 wt.%)	HDPE	2-Roll mill-Press	2890(60)	36.88(1.10)	4.60(0.10)
[2]		NHDPE [6]	2-Roll mill-Press	1170(170)	21.39(0.34)	7.80(0.51)
[2]	Birch fibers (10 wt.%)	NHDPE	2-Roll mill-Press	1930(160)	26.89(1.03)	4.00(0.94)
[2]	Birch fibers (10 wt.%) + MAPE (3 wt.%)	NHDPE	2-Roll mill-Press	1990(180)	27.21(0.55)	3.19(0.31)
[2]	Birch fibers (30 wt.%)	NHDPE	2-Roll mill-Press	3040(290)	33.47(3.13)	2.18(0.35)

Table 4. *Cont.*

Ref	Fiber Type and Content	Matrix	Fabrication Method [1]	Modulus of Elasticity (MPa)	Tensile Strength (MPa)	Strain at Break (%)
[2]	Birch fibers (30 wt.%) + MAPE (3 wt.%)	NHDPE	2-Roll mill-Press	3500(130)	40.60(1.37)	2.50(0.03)
[1]		BioFlex (0.5–0.7 mm) [2]	Extrusion-Press	142	10.7	123
		BioFlex [6]	Re-processed	143	10.1	99
[1]	Beech wood flour (15 wt.%)	BioFlex	Extrusion-Press	313	9.2	12.9
	Beech wood flour (15 wt.%)	BioFlex	Re-processed	300	8.9	11.5
[1]	Beech wood flour (30 wt.%)	BioFlex	Extrusion-Press	539	11.2	6.6
	Beech wood flour (30 wt.%)	BioFlex	Re-processed	477	10.8	7.3
[44] [4,5]		Nylon-MXD6 [6] (15 µm) [2]	Biaxial stretch	3800(385)	220(22)	75
[44] [4,5]		Nylon 6 (15 µm) [2]	Biaxial stretch	1700(170)	200(20)	90
[44] [4,5]		PET [6] (15 µm) [2]	Biaxial stretch	3400(350)	160(16)	140
[46] [3,4]		PVC [6] (12 µm) [2,5]		120 ± 20	42 ± 7	35 ± 5
[46] [3,4]	Montmorillonite	Cassava starch (71 µm) [2]		1100 -1200	21–25	1082–2000
[46] [3,4]		Chitosan+ PLA [6] (67 µm) [2]		17–11	30–25	165 ± 7

[1] compounding –specimen fabrication method. [2] reported thickness. [3] for food packaging applications. [4] values are cited in the reference. [5] commercially available. [6] CO = cotton, CE = cellulose, HCE = hydrolyzed-cellulose, AS = almond skin, ASF = almond shell flour, PBS = poly(butylene succinate), MLO = maleinized linseed oil, PP-g-MA = polypropylene-graft-maleic anhydride, PP = polypropylene, HDPE = high density polyethylene, LDPE = low density polyethylene, PC = polycarbonate, LLDPE = linear low density polyethylene, NPE = natural high density polyethylene, MAPE = maleated polyethylene coupling agent, BioFlex = commercial blend of PLA and Thermoplastic-Copolyesters (TPC), nylon-MXD6 = poly(m-xylylene adipamide), PET = poly(ethylene terephthalate), PVC = poly(vinyl chloride), PLA = poly(lactic acid). Note: data are cited as reported in the respective references.

To study the surface hydrophobicity of the PCL/SD WPCs as a function of SD content, water contact angles were measured. Figure 10 shows sample sessile drops on studied composite surfaces. Table 5 summarizes the results. Neat PCL sheet surfaces had WCAs averaging about 57°, implying partial wetting. In general, contrary to predictions, the addition of SD increased the WCA, implying increasing hydrophobicity despite the hydrophilic nature of wood, this is attributed to higher surface roughness with addition of SD. Addition of SD beyond 30 wt.% resulted in a lowering of the WCA, this is attributed to increasing amounts of the hydrophilic SD on the surface.

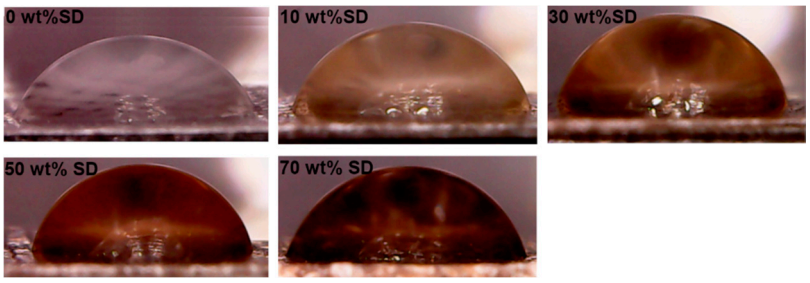

Figure 10. Sample sessile drops on PCL/SD composites as function of SD content for water contact angle measurement.

Table 5. Average measured static water contact angle on cryomilled composite sheets as function of SD content.

Wood Content (wt.%)	0	10	30	50	70
Water Contact Angle (°)	57 (1)	78 (5)	88 (11)	81 (2)	71 (7)

4. Conclusions

Recent trends in consumer markets are moving towards greener packaging. The present study investigated solid-state cryomilling for compounding PCL with SD to produce WPC sheets for greener packaging applications. It was evident that solid-state compounding places no restriction on the SD content compared to melt-blending techniques, however, the limitation is set by the final product processing, properties, and potential application. Optical imaging and SEM revealed the efficient grinding and compounding capacity of cryomilling, with images indicating uniform distribution of SD in the PCL matrix even at high SD content. Tensile strength and elongation at break of the composites decreased with increasing SD content, however, cryomilling resulted in higher ductility than extrusion. The modulus of elasticity significantly increased. Water contact angles implied partial wettability of the composites, with PCL covering SD particles. Visual inspections, as well as TGA, did not indicate any significant degradations during processing. In conclusion, PCL/SD WPC may be a potential green candidate for packaging applications. Future research will investigate the fabrication of PCL-SD WPC bags via blow molding as a commercial processing technique for manufacturing flexible bags.

Author Contributions: Conceptualization; methodology and formal analysis, R.M.A.; investigation, R.M.A. and M.F.; writing, R.M.A. All authors have read and agreed to the published version of the manuscript.

Funding: This research was funded by the German Jordanian University Deanship of Graduate Studies and Scientific Research.

Acknowledgments: The authors would like to acknowledge the following students for assistance in sample preparation and testing: Ahmad Hijazi, Ahmad Saleh, Mohammad Naser, Mohammad AlAqtash, and Edward Qassar. The authors would also like to thank Perstorp Group for kindly supplying the Capa® 6506.

Conflicts of Interest: The authors declare no conflict of interest.

References

1. Morreale, M.; Liga, A.; Mistretta, M.C.; Ascione, L.; La Mantia, F.P. Mechanical; thermomechanical and reprocessing behavior of green composites from biodegradable polymer and wood flour. *Materials* **2015**, *8*, 7536–7548. [CrossRef]
2. Bravo, A.; Toubal, L.; Koffi, D.; Erchiqui, F. Development of novel green and biocomposite materials: Tensile and flexural properties and damage analysis using acoustic emission. *Mater. Des.* **2015**, *66*, 16–28. [CrossRef]
3. Abdulkhani, A.; Hosseinzadeh, J.; Ashori, A.; Dadashi, S.; Takzare, Z. Preparation and characterization of modified cellulose nanofibers reinforced polylactic acid nanocomposite. *Polym. Test.* **2014**, *35*, 73–79. [CrossRef]
4. Cavdar, A.D.; Mengeloglu, F.; Karakus, K. Effect of boric acid and borax on mechanical; fire and thermal properties of wood flour filled high density polyethylene composites. *Meas. J. Int. Meas. Confed.* **2015**, *60*, 6–12. [CrossRef]
5. Rajak, D.K.; Pagar, D.D.; Menezes, P.L.; Linul, E. Fiber-reinforced polymer composites: Manufacturing; properties; and applications. *Polymers* **2019**, *11*, 1667. [CrossRef]
6. Geyer, R.; Jambeck, J.R.; Law, K.L. Production, use, and fate of all plastics ever made. *Sci. Adv.* **2017**, *3*, e1700782. [CrossRef]
7. Berthet, M.A.; Angellier-Coussy, H.; Chea, V.; Guillard, V.; Gastaldi, E.; Gontard, N. Sustainable food packaging: Valorising wheat straw fibres for tuning PHBV-based composites properties. *Compos. Part A Appl. Sci. Manuf.* **2015**, *72*, 139–147. [CrossRef]
8. Fazita, M.R.N.; Jayaraman, K.; Bhattacharyya, D.; Hossain, M.S.; Haafiz, M.K.M.; Abdul Khalil, H.P.S. Disposal options of bamboo fabric-reinforced poly(lactic) acid composites for sustainable packaging: Biodegradability and recyclability. *Polymers* **2015**, *7*, 1476–1496. [CrossRef]

9. Johansson, C.; Bras, J.; Mondragon, I.; Nechita, P.; Plackett, D.; Simon, P.; Svetec, D.G.; Virtanen, S.; Baschetti, M.G.; Breen, C.; et al. Renewable fibers and bio-based materials for packaging applications—A review of recent developments. *BioResources* **2012**, *7*, 2506–2552. [CrossRef]
10. Van den Broek, L.A.M.; Knoop, R.J.I.; Kappen, F.H.J.; Boeriu, C.G. Chitosan films and blends for packaging material. *Carbohydr. Polym.* **2015**, *116*, 237–242. [CrossRef] [PubMed]
11. Jamshidian, M.; Tehrany, E.A.; Imran, M.; Jacquot, M.; Desobry, S. Poly-lactic acid: Production, applications, nanocomposites, and release studies. *Compr. Rev. Food Sci. Food Saf.* **2010**, *9*, 552–571. [CrossRef]
12. Armentano, I.; Bitinis, N.; Fortunati, E.; Mattioli, S.; Rescignano, N.; Verdejo, R.; Lopez-Manchado, M.A.; Kenny, J.M. Multifunctional nanostructured PLA materials for packaging and tissue engineering. *Prog. Polym. Sci.* **2013**, *38*, 1720–1747. [CrossRef]
13. Ahmed, J.; Varshney, S.K. Polylactides-chemistry, properties and green packaging technology: A review. *Int. J. Food Prop.* **2011**, *14*, 37–58. [CrossRef]
14. Eng, C.C.; Ibrahim, N.A.; Zainuddin, N.; Ariffin, H.; Yunus, W.M.Z.W.; Then, Y.Y.; Teh, C.C. Enhancement of mechanical and thermal properties of polylactic acid/polycaprolactone blends by hydrophilic nanoclay. *Indian J. Mater. Sci.* **2013**, *2013*, 1–11. [CrossRef]
15. Bhatia, A.; Gupta, R.K.; Bhattacharya, S.N.; Choi, H.J. Compatibility of biodegradable poly (lactic acid) (PLA) and poly (butylene succinate) (PBS) blends for packaging application. *Korea Aust. Rheol. J.* **2007**, *19*, 125–131.
16. Khan, R.A.; Beck, S.; Dussault, D.; Salmieri, S.; Bouchard, J.; Lacroix, M. Mechanical and barrier properties of nanocrystalline cellulose reinforced poly(caprolactone) composites: Effect of gamma radiation. *J. Appl. Polym. Sci.* **2013**, *129*, 3038–3046. [CrossRef]
17. Ludueña, L.; Vázquez, A.; Alvarez, V. Effect of lignocellulosic filler type and content on the behavior of polycaprolactone based eco-composites for packaging applications. *Carbohydr. Polym.* **2012**, *87*, 411–421. [CrossRef]
18. García, A.V.; Santonja, M.R.; Sanahuja, A.B.; Selva, M.D.C.G. Characterization and degradation characteristics of poly(ε-caprolactone)-based composites reinforced with almond skin residues. *Polym. Degrad. Stab.* **2014**, *108*, 269–279. [CrossRef]
19. Dwivedi, R.; Kumar, S.; Pandey, R.; Mahajan, A.; Nandana, D.; Katti, D.S.; Mehrotra, D. Polycaprolactone as biomaterial for bone scaffolds: Review of literature. *J. Oral Biol. Craniofacial Res.* **2020**, *10*, 381–388. [CrossRef]
20. Mohamed, R.M.; Yusoh, K. A review on the recent research of polycaprolactone (PCL). *Adv. Mater. Res.* **2015**, *1134*, 249–255. [CrossRef]
21. Guarás, M.P.; Alvarez, V.A.; Ludueña, L.N. Processing and characterization of thermoplastic starch/polycaprolactone/compatibilizer ternary blends for packaging applications. *J. Polym. Res.* **2015**, *22*, 1–12. [CrossRef]
22. Ahmed, J.; Mulla, M.; Jacob, H.; Luciano, G.; Bini, T.B.; Almusallam, A. Polylactide/poly(ε-caprolactone)/zinc oxide/clove essential oil composite antimicrobial films for scrambled egg packaging. *Food Packag. Shelf Life* **2019**, *21*, 1–9. [CrossRef]
23. Joseph, C.S.; Prashanth, K.V.H.; Rastogi, N.K.; Indiramma, A.R.; Reddy, S.Y.; Raghavarao, K.S.M.S. Optimum blend of chitosan and poly-(ε-caprolactone) for fabrication of films for food packaging applications. *Food Bioprocess Technol.* **2011**, *4*, 1179–1185. [CrossRef]
24. Wu, C.-S. Analysis of mechanical; thermal; and morphological behavior of polycaprolactone/wood flour blends. *J. Appl. Polym. Sci.* **2004**, *94*, 1000–1006. [CrossRef]
25. Karakus, K.; Mengeloglu, F. Polycaprolactone (PCL) based polymer composites filled wheat straw flour. *Kast. Univ. J. For. Fac.* **2016**, *16*, 264–268. [CrossRef]
26. Dhakal, H.N.; Ismail, S.O.; Zhang, Z.; Barber, A.; Welsh, E.; Maigret, J.-E.; Beaugrand, J. Development of sustainable biodegradable lignocellulosic hemp fiber/polycaprolactone biocomposites for light weight applications. *Compos. Part A Appl. Sci. Manuf.* **2018**, *113*, 350–358. [CrossRef]
27. Follain, N.; Belbekhouche, S.; Bras, J.; Siqueira, G.; Chappey, C.; Marais, S.; Dufresne, A. Tunable gas barrier properties of filled-PCL film by forming percolating cellulose network. *Colloids Surf. A Physicochem. Eng. Asp.* **2018**, *545*, 26–30. [CrossRef]
28. Martínez-Abad, A.; Sánchez, G.; Fuster, V.; Lagaron, J.M.; Ocio, M.J. Antibacterial performance of solvent cast polycaprolactone (PCL) films containing essential oils. *Food Control* **2013**, *34*, 214–220. [CrossRef]
29. Dhakal, H.; Bourmaud, A.; Berzin, F.; Almansour, F.; Zhang, Z.; Shah, D.U.; Beaugrand, J. Mechanical properties of leaf sheath date palm fibre waste biomass reinforced polycaprolactone (PCL) biocomposites. *Ind. Crop. Prod.* **2018**, *126*, 394–402. [CrossRef]

30. Najafi, S.K.; Hamidinia, E.; Tajvidi, M. Mechanical properties of composites from sawdust and recycled plastics. *J. Appl. Polym. Sci.* **2006**, *100*, 3641–3645. [CrossRef]
31. Rahman, K.-S.; Islam, M.; Rahman, M.; Hannan, M.; Dungani, R.; Khalil, H. Flat-pressed wood plastic composites from sawdust and recycled polyethylene terephthalate (PET): Physical and mechanical properties. *SpringerPlus* **2013**, *2*, 629–636. [CrossRef] [PubMed]
32. Smith, A.P.; Spontak, R.J.; Ade, H.; Smith, S.D.; Koch, C.C. High-energy cryogenic blending and compatibilizing of immiscible polymers. *Adv. Mater.* **1999**, *11*, 1277–1281. [CrossRef]
33. Smith, A.P.; Spontak, R.J.; Ade, H. On the similarity of macromolecular responses to high-energy processes: Mechanical milling vs. irradiation. *Polym. Degrad. Stab.* **2001**, *72*, 519–524. [CrossRef]
34. Vertuccio, L.; Gorrasi, G.; Sorrentino, A.; Vittoria, V. Nano clay reinforced PCL/starch blends obtained by high energy ball milling. *Carbohydr. Polym.* **2009**, *75*, 172–179. [CrossRef]
35. Jia, S.; Yu, D.; Zhu, Y.; Wang, Z.; Chen, L.; Fu, L. Morphology, crystallization and thermal behaviors of PLA-based composites: Wonderful effects of hybrid GO/PEG via dynamic impregnating. *Polymers* **2017**, *9*, 528. [CrossRef] [PubMed]
36. Lebourg, M.; Serra, R.S.; Estellés, J.M.; Sánchez, F.H.; Ribelles, J.G.; Antón, J.S. Biodegradable polycaprolactone scaffold with controlled porosity obtained by modified particle-leaching technique. *J. Mater. Sci. Mater. Med.* **2008**, *19*, 2047–2053. [CrossRef] [PubMed]
37. Panthapulakkal, S.; Sain, M. Preparation and characterization of cellulose nanofibril films from wood fibre and their thermoplastic polycarbonate composites. *Int. J. Polym. Sci.* **2012**, *2012*, 1–6. [CrossRef]
38. Banat, R.; Fares, M.M. Thermo-gravimetric stability of high density polyethylene composite filled with olive shell flour. *Am. J. Polym. Sci.* **2015**, *5*, 65–74.
39. Liminana, P.; Quiles-Carrillo, L.; Boronat, T.; Balart, R.; Montanes, N. The effect of varying almond shell flour (ASF) loading in composites with poly(butylene succinate (PBS) matrix compatibilized with maleinized linseed oil (MLO). *Materials* **2018**, *11*, 2179. [CrossRef]
40. Khan, A.; Khan, R.A.; Salmieri, S.; Le Tien, C.; Riedl, B.; Bouchard, J.; Chauve, G.; Tan, V.; Kamal, M.R.; Lacroix, M. Mechanical and barrier properties of nanocrystalline cellulose reinforced chitosan based nanocomposite films. *Carbohydr. Polym.* **2012**, *90*, 1601–1608. [CrossRef]
41. Arbelaiz, A.; Fernández, B.; Valea, A.; Mondragon, I. Mechanical properties of short flax fibre bundle/poly(ε-caprolactone) composites: Influence of matrix modification and fibre content. *Carbohydr. Polym.* **2006**, *64*, 224–232. [CrossRef]
42. Jiménez, A.; Ruseckaite, R.A. Binary mixtures based on polycaprolactone and cellulose derivatives: Thermal degradation and pyrolysis. *J. Therm. Anal. Calorim.* **2007**, *88*, 851–856. [CrossRef]
43. Annandarajah, C.; Li, P.; Michel, M.; Chen, Y.; Jamshidi, R.; Kiziltas, A.; Hoch, R.; Grewell, D.; Montazami, R. Study of agave fiber-reinforced biocomposite films. *Materials* **2018**, *12*, 99. [CrossRef] [PubMed]
44. Niaounakis, M. Polymers used in flexible packaging. In *Recycling of Flexible Plastic Packaging*, 1st ed.; Elsevier Inc.: Amsterdam, The Netherlands, 2020; pp. 57–96.
45. Majeed, K.; Jawaid, M.; Hassan, A.; Abu Bakar, A.; Abdul Khalil, H.P.S.; Salema, A.A.; Inuwa, I. Potential materials for food packaging from nanoclay/natural fibres filled hybrid composites. *Mater. Des.* **2013**, *46*, 391–410. [CrossRef]
46. Abdul Khalil, H.P.S.; Banerjee, A.; Saurabh, C.K.; Tye, Y.Y.; Suriani, A.B.; Mohamed, A.; Karim, A.A.; Rizal, S.; Paridah, M.T. Biodegradable films for fruits and vegetables packaging application: Preparation and properties. *Food Eng. Rev.* **2018**, *10*, 139–153. [CrossRef]

Publisher's Note: MDPI stays neutral with regard to jurisdictional claims in published maps and institutional affiliations.

© 2020 by the authors. Licensee MDPI, Basel, Switzerland. This article is an open access article distributed under the terms and conditions of the Creative Commons Attribution (CC BY) license (http://creativecommons.org/licenses/by/4.0/).